Phys. Status Solidi B **251**, No. 10, 2061–2066 (2014) / **DOI** 10.1002/pssb.201350242

Part of Special Issue on
Ferroic Glasses: Magnetic, Polar and Strain Glass

physica status solidi b
www.pss-b.com
basic solid state physics

Invited Article

Domain glass

E. K. H. Salje[*,1], **X. Ding**[2], **and O. Aktas**[1]

[1] Department of Earth Sciences, University of Cambridge, Cambridge, UK
[2] State Key Laboratory for Mechanical Behavior of Materials, Xi'an Jiaotong University, Xi'an 710049, P. R. China

Received 30 September 2013, revised 10 December 2013, accepted 12 December 2013
Published online 22 January 2014

Keywords domain glass, ergodic structures, ferroelastic domains, Vogel–Fulcher dynamics

* Corresponding author: e-mail ekhard@esc.cam.ac.uk, Phone: +44 1223 768321, Fax: +44 1223 33450

Microstructural patterns of twin boundaries and tweed in ferroelastic materials display typical aspects of glasses. The patterns are complex, their dynamics follows Vogel–Fulcher statistics and their field cooling–non-field cooling hysteresis is similar to those described in this issue as 'strain glasses'. The difference is that domain glasses do not need extrinsic defects to form. In the paraelastic phase, an intrinsic tweed pattern dominates the high temperature precursor regime. Experimentally, massive elastic precursor softening is related to polar standing waves, which are attributed to the glassy relaxation of the tweed pattern. In the ferroelastic phase we find a complex twin pattern when the sample is strained with a constant strain rate. The dynamics of the pattern formation is a-thermal at low temperatures and follows Vogel–Fulcher statistics at moderately high temperatures. It is argued that domain boundary patterns can hence evolve glass-like states while the underlying matrix remains fully crystalline without any defect induced disorder.

1 Introduction Non-ergodic, glass like structures are commonly observed whenever the degree of disorder in a structural phase transition is large. Non-ergodicity is the defining quantity in relaxor materials [1–3] but it is not known how the breaking of ergodicity occurs in the limiting case of weakly disordered systems. Decreasing the strength of the random field in a ferroic phase transition will make the transition increasingly more ergodic and one may be tempted to assume that the fully ordered system undergoes a 'classic' phase transition without any ergodicity breaking. It is not clear whether the transition between relaxor-type, non-ergodic behaviour and an ergodic, ferroic transition mechanism is stepwise or continuous. Ren and collaborators [4] have argued that an abrupt transition exists between the long range ordered state and the non-ergodic glass state. Nevertheless, even for weak disorder, the ferroic state contains significant fluctuations of the order parameter and relaxor type behaviour cannot be excluded. Lloveras et al. [5] have shown that spatially heterogeneous states that occur in ferroelastic transitions depend crucially on the elastic anisotropy with tweed type microstructures for anisotropic interactions and mottled structures with almost spherical nano domains for isotropic interactions (e.g. in NiTi). They argue that such microstructures lead to structural disorder that gives rise to a distribution of energy barriers that, when overcoming a well-defined threshold, screen the long-range interactions and suppress the structural phase transition. They clearly identified the thermal precursor interval at temperatures just above the transition point as the key thermal regime where disorder based features can be identified most clearly.

In this paper, we follow a similar argument. We address an extreme situation where the amount of extrinsic disorder is vanishingly small compared with the local disorder generated by intrinsic fluctuations of the order parameter. In other words, we are dealing with defect free systems (in computer simulations) or with materials that contain no or a very small defect concentration (experimentally). We could expect such systems to be fully ergodic but find experimentally some glass-like features. The glassiness is not related to the structural matrix, however, but entirely to ferroelastic or ferroelectric microstructures. In this sense we extend the concept of domain boundary engineering [6, 7] to show that the subsystem of domain boundaries and their precursors can themselves form glass states while the underlying matrix remains fully crystalline.

Previous experimental studies that inspired this idea include Potassium Tantalate Niobate (KTN) with high Nb content where the transition is expected to follow the classic ferroelectric transition mechanism. Dielectric relaxations were found not to be (fully) ergodic, however, and jump correlations were found in dielectric spectroscopy [8]. Similarly, elastic relaxations in ferroelastic $LaAlO_3$ show low frequency

resonances which are highly broadened with a stretching exponent of the Cole–Cole relaxation of $\mu \approx 0.6$ [9]. Such exponents measure the deviation from a Debye relaxation ($\mu = 1$) and have been linked to the appearance of broken ergodicity [10]. Recent work on $PbSc_{0.5}Ta_{0.5}O_3$ (PST) has shown that the ferroelectric transition has all the hallmarks of a classic ferroelectric and/or ferroelastic phase transition together with huge precursor polarity that exists in the nominally cubic phase at temperatures just above the ferroelectric transition point [11]. Glassiness in nominally defect free materials was previously observed in single crystals of C_{60} and similar compounds [12].

The decay of ergodicity of ferroelastic phase transitions near the clean limit is somewhat akin to the plateau effect of chemical mixing [13]. Mixed systems show no effect of mixing on the averaged transition temperature of a displacive phase transition for small defect concentrations (while the transition may smear out and local field effects may become important). Large concentrations of dopant atoms can lead to ideal chemical mixing, and paradoxically a 'clean' transition occurs when long range strain effects dominate the transition mechanism. The transition temperature is now dependent on the dopant concentration while a temperature plateau is observed when the dopant concentration is small. The edge of the plateau indicates the threshold level of dopant concentration that is needed to homogenize the doping effect [14–17].

The average distance between the dopants at this point gives an estimate for the interaction length between the dopants, which can vary between a few nm and some 100 nm. We argue in this paper that no extrinsic dopants are required in the case of glassy precursor behaviour of ferroelastic materials and in jammed domain structures so that the glassiness (and weak or broken ergodicity) can be an intrinsic feature of a ferroelastic phase transition. In our experiments and simulations we remain firmly inside the plateau regime of chemical mixing.

2 Glassy precursor effects in improper ferroelastics and polarity in a non-polar matrix Improper ferroelastics are defined as ferroelastic materials where the order parameter of the transition is neither the strain (which would be a proper ferroelastic) nor is there a bi-linear coupling between the order parameter and the strain (which would be a pseudo-proper ferroelastic). An improper ferroelastic shows no elastic softening in the precursor regime related to fluctuations of the order parameter and are hence ideal for the investigation of softening mechanisms that are unrelated to fluctuations of the order parameter [18]. The same argument is true for co-elastic materials [19] and the first experimental observation of unexpected precursor softening in co-elastic quartz dates back to 1970 [20]. Axe and Shirane correctly argued that the elastic anomaly is related to a low frequency Raman-active mode in the high temperature phase, which is not the structural soft mode. This argument was formalized and extended by Carpenter and Salje [18] who showed that any low frequency mode $\omega(k)$, where k is a wave vector in reciprocal space, would dynamically soften elastic moduli even though this mode is not itself the structural soft mode. The key argument here is that the precursor softening ΔC depends on the dispersion of the phonon branch. As the integral over the dispersion curve needs to extend only over the phonon branches with small values of $\omega(k)$ one finds that the precursor effect depends crucially on the dimensionality of the k-integration. With a parabolic dispersion relation $\omega^2(k) = \epsilon^2(1 + \sum_{i=x,y,z} c_i^2 k_i^2)$, where ϵ and c are proportionality constants, the integral depends on the dimension, d, of the soft phonon branch. The most common cases are three one-dimensional low-lying branches with $d = 3$ and two-dimensional branches with $d = 2$. If a temperature scaling of ϵ is assumed to be similar to a non-critical soft mode, $\epsilon^2 = \epsilon_{\min}^2 + A|T - T_c|$, where A is a constant and T_c is a critical temperature, (taking $\epsilon \propto 1/c$) the temperature evolution of the precursor softening for the elastic constant C is given by $\Delta C \propto |T - T_c|^{-0.5}$ for 3 low-lying branches in three dimensions, $\Delta C \propto |T - T_c|^{-1}$ for 2 low-lying branches in a plane and $\Delta C \propto |T - T_c|^{-1.5}$ for a single low frequency branch. The exponents are usually called κ with $\kappa = -0.5$, $\kappa = -1$, $\kappa = -1.5$, respectively. In quartz one expects by symmetry a planar degeneracy and, indeed, a value of $\kappa = -1$ was observed [20]. Similarly, the symmetry reduction from cubic to rhombohedral in $LaAlO_3$ also may involve planar degeneracy and a value of κ close to unity was reported in Ref. [21]. In most other cases of phase transitions in ferroelastic perovskite structures such as $BaTiO_3$ and $SrTiO_3$, the transition from the cubic to the tetragonal structure involves 3 soft branches with a best fit of the experimental data to $\kappa = -0.5$. Large precursor softening in $KMnF_3$ with $\kappa = -0.5$ was reported in Refs. [22, 23].

The magnitude of the elastic precursor softening varies largely between compounds with relatively little precursor softening in $LaAlO_3$ [21] and $SrTiO_3$ [24]. The other extreme case is observed in $BaTiO_3$ where a massive precursor softening occurs in the cubic phase with some 25% reduction of the modulus [25]. The massive softening extends over a temperature range of ca. 200 K. It is hard to understand why so large precursor effects exist in $BaTiO_3$ while the effect remains very small in structurally closely related $SrTiO_3$. The solution to this riddle may be related to the observation that the precursor phase in $BaTiO_3$ is much more complex than in the other materials: the phase is polar [26] while the cubic symmetry $Pm\bar{3}m$ disallows any such polar behaviour. In addition, we find that an equally good (or even better) fit of the observed temperature evolution of the moduli can be obtained with a thermally activated Vogel–Fulcher process with $\Delta C \propto \exp(E_a/|T - T_{VF}|)$ [25]. In this equation, the Vogel–Fulcher temperature, T_{VF}, is below the transition temperature and the activation energy, E_a, corresponds to the typical hopping energy of local 'defects' such as disordered Ti positions which are slightly shifted from the midpoints of the TiO_6 octahedra in $BaTiO_3$. Large (precursor) elastic softening was also observed in PST [11] where polar precursors were again observed in the cubic paraelastic phase. The temperature evolution of the precursor softening in PST

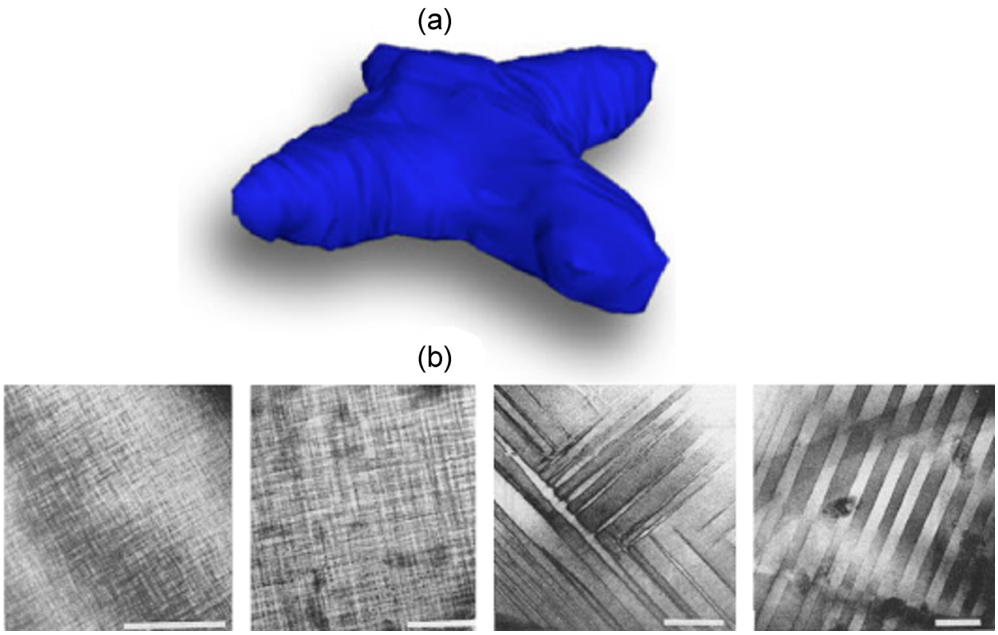

Figure 1 Simulation of a tweed diffraction pattern for Co-doped $YBa_2Cu_3O_7$ in the upper panel is shown as four-armed starfish and clearly indicates the elastically soft directions where fluctuations are largest (after [32]. Copyright (2012), AIP Publishing LLC). Lower panel shows transmission electron micrographs of tweed (left 2) and twin (right 2) patterns observed in Co-doped $YBa_2Cu_3O_7$ above and below the transition point, respectively (after Ref. [31], reprinted by permission of the publisher: Taylor & Francis Ltd, http://www.tandf.co.uk/journals. The scale bar in the transmission electron microscope images is 100 nm.

complies both with the power law scaling ($\kappa = -0.5$) and the Vogel–Fulcher law. No attempt was made by Salje and Zhang to compare the precursor softening in $KMnF_3$ with a Vogel–Fulcher equation but the close similarity between the power law fit and the exponential function over a limited temperature interval makes it likely that both approaches would yield equally good results. The large amplitude of the softening was also related to the existence of local defects in $KMnF_3$ with migration activation energies in the range of 0.17–0.23 eV [23].

The empirical observation is hence that large precursor softening is a fingerprint for Vogel–Fulcher processes while weak softening may be related to phonon coupling between low frequency phonons and the elastic moduli. Both interpretations have in common that the elastic moduli couple with dynamic excitations. The difference between the two processes is the nature of the coupled excitations: they are either vibrational with relatively high frequencies or relaxational with much lower frequencies. The relaxational processes and their Vogel–Fulcher dynamics imply the glass dynamics of the elastic softening and we will now discuss how such glass states may be modelled. Let us start with a model where the local dynamical variable is a spin-type variable S_i such as the off-centring of Ti inside the ith oxygen cage in $BaTiO_3$ [27]. The interaction between the S_i is twofold: close neighbours can interact directly while others will interact elastically. In the cubic phase we have no spontaneous deformation of the sample so that all interactions are related to local displacements in the cubic lattice. The Gibbs free energy of the cubic phase can then be derived from a local Hamiltonian which was introduced in the 1990s [28–31] to describe the effect of non-local strain interactions in Ising models. The entropy of the system is mainly related to the spin variable while the interactions are strain related. The superposition of these two effects leads to microstructures of a fine mesh of deformations which are named 'tweed'. Typical tweed structures (the structure factor and the real image) are shown in Fig. 1. Note that the tweed structure is dynamic in the absence of defect pinning in the paraelastic phase while the image in Fig. 1 relates to a pinned tweed structure in Co-doped $YBa_2Cu_3O_7$ [31]. Twin structures (right two images) of Co-doped $YBa_2Cu_3O_7$ that occur below the transition temperature are also shown in Fig. 1b (right two images) for comparison.

The tweed pattern in the paraelastic phase stems from the fluctuations of the order parameter Q_i: $S_k = \langle Q_k Q_{-k} \rangle$ with k being the position in reciprocal space and Q_k is the Fourier transform of the local state parameter $Q(R)$ at position R which in our example measures the deviation of the order/disorder component from its zero value at $T \gg T_c$ (e.g. the off-centring of Ti in an oxygen octahedron). Using the tweed Hamiltonian in the Bratkovsky, Heine and Salje, BHS, model [33] one can show that the intrinsic elastic moduli do not change by tweed formation in the harmonic approximation. On the other hand, the tweed becomes more accentuated when the temperature approaches the transition temperature from above as S_k increases with decreasing temperature as $S_k = k_B T/(k_B T - J_k)$ where the exchange interaction scales as $\boldsymbol{J}_k = d(\boldsymbol{n}) - g(\boldsymbol{n})\boldsymbol{k}^2$, where $\boldsymbol{n} = \boldsymbol{k}/k$ is a directional unit vector. The functions d and g

depend only on angular functions and can be derived from the symmetry of the interactions. The functional form of J_k is usually a fourfold clover as shown in the diffraction pattern in Fig. 1 [32].

The reduction of the elastic moduli in the precursor regime due to the tweed formation requires interactions that go beyond the BHS model. Two mechanisms are plausible. First, the regions of vanishing order parameters of the tweed (equivalent to regions of high spatial gradients and hence flexoelectric effects) will display reduced moduli. This idea was explored in Ref. [34] and it was shown that twin boundaries in $CaTiO_3$ compress under stress by some 2% more than the equivalent bulk material. The size of the effect in the actual tweed regime is not known but can be expected to be of a similar magnitude as in twin microstructures. This effect appears to be too small to account for the observed massive elastic precursor softening. The second and larger effect is expected to stem from the relaxation of the tweed pattern and relates directly to its glass-like behaviour. Computer simulations of a simple model have shown that tweed microstructures occur under weak shear stress and result in local relaxations that reduce the elastic stiffness of the system [35].

Comparing the results in Ref. [35] (their Fig. 4) with the quadratic increase of the local potential energy with increasing strain (the curvature is the appropriate elastic modulus) shows that the elastic energy is significantly reduced at high temperatures and that strain relaxations follow a Vogel–Fulcher statistics rather than a power law as seen at low temperatures [32]. Vogel–Fulcher statistics and stretched exponential laws are also commonly observed in dynamically strained ferroelastics in their elastic regime [36, 37]. The proposed physical process leading to a massive elastic precursor in ferroelastic, martensitic, and ferroelectric materials is hence related to the formation of precursor tweed microstructures. These tweed structures have glass-like, non-ergodic features and show softening due to relaxational modes, which are absent in the low temperature ferroic phase. Glass like features in materials with massive precursor softening are well observed at temperatures above the transition point while their existence does not imply that the ferroic phase itself is non-ergodic or glassy.

3 Jamming and glassy behaviour in strained ferroelastics We now consider ferroic materials in their ferroic state. The stress-free material defines a thermodynamic ground state and, in the case of ferroelastics, their physical behaviour can be derived to an excellent approximation by Landau theory. The microstructural ground state is the single crystal if no forces or specific boundary conditions (e.g. clamping) are applied. The energy of a twin boundary [6] is similar to that of a surface layer in the order of $0.1\ \mathrm{J\,m^{-2}}$. This situation changes fundamentally when the material is sheared. Increasing shear will lead to a yield point collapse at which the sample is shattered into a multitude of domain states while the macroscopic integrity of the sample (usually) remains intact. If no further strains are applied we find that the microstructures remain 'stranded' which means that they will not change even if other parameters do. This is the reason why such microstructures are so important in mineralogy: once a microstructure has been formed in geological history they will remain constant over geological times. Some of these microstructures are known to have survived more than one billion years in the geological environment although the microstructure does not represent an energy minimum under free boundary conditions [38]. In the context of device applications, the application of domain boundaries my equally generate domain patterns which are long lived and which allow the functionality of the device [39].

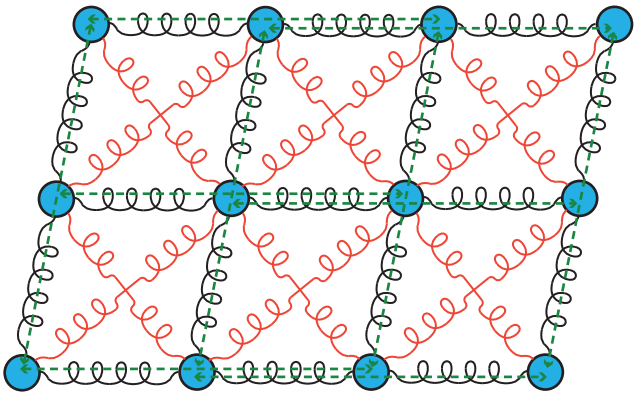

Figure 2 Interatomic potential for a generic ferroelastic model. The model contains nearest-neighbour (black springs), next-nearest-neighbour (red springs), and third-nearest-neighbour (green lines) interactions. See text for description of the model (after Ref. [41]. Copyright (2013), AIP Publishing LLC).

Glass-like structures are generated when the driving forces are very large. A typical example is the stress induced twinning at low temperatures. These twin patterns involve a very high number of twin intersections and are distinctly different from stripe patterns which are generated under weak strain fields when the sample is cooled slowly through the ferroelastic transition point. Field cooling and non-field cooling give very different pattern formation. We will now discuss how the complexity and glass dynamics of a strained pattern can lead to states, which have all the hallmarks of weak ergodicity. A simple model Hamiltonian for the creation of domain structures was introduced in Ref. [35] and is depicted in Fig. 2. Nearest-neighbour (black springs), next-nearest-neighbour (red springs), and third-nearest-neighbour (green lines) interactions included in the model ensures a spontaneous shear of the unit cells. The springs between the nearest-neighbours and third-nearest neighbours define the elastic background and define the thickness of interfaces. The red Landau springs (interaction between next-nearest neighbours) define the double well potential of the ferroelastic phase transition (see Ref. [35]). They define a second order phase transition inspired by the transition of $SrTiO_3$ (Ref. [40]). The interatomic interaction of this potential is listed as follows: $V_{\mathrm{hard}}(r) = 20(r-1)^2$

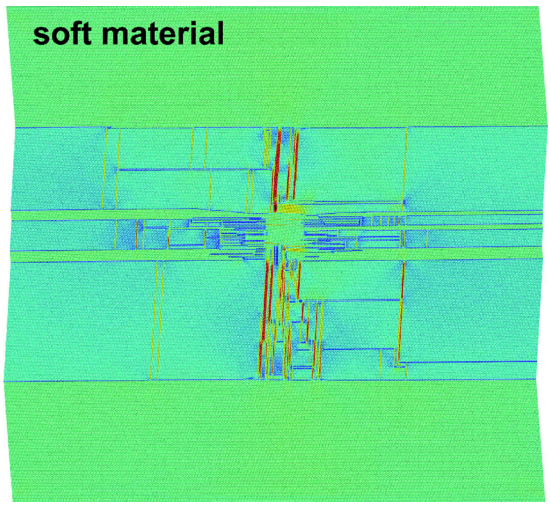

Figure 3 Microstructure under shear above the yield point in the model system in Fig. 2. The potential corresponds to a soft system; hard systems show slightly more dilute twin structures (after Ref. [32]. Copyright (2012), AIP Publishing LLC).

and $V_{\text{soft}}(r) = 10(r-1)^2$ $(0.8 < r < 1.2)$, $V(r) = -10(r-2)^2 + 2000(r-2)^4$ $(1.207 < r < 1.621)$, $V(r) = -(r-2)^4$ $(1.8 < r < 2.2)$.

Using this model, it has been shown that the ensuing domain patterns are size dependent when the sample comprises less than 200 particles in one direction [41]. Samples with $>$ 1 million particles in two-dimensional simulations showed no such size dependence and can be analyzed as a characteristic twin pattern under strain at conditions far from equilibrium, an example of which is presented in Fig. 3 for a soft system ($YBa_2Cu_3O_7$) [32]. A simulated diffraction pattern of twins for such a soft system is shown in Fig. 4 [32].

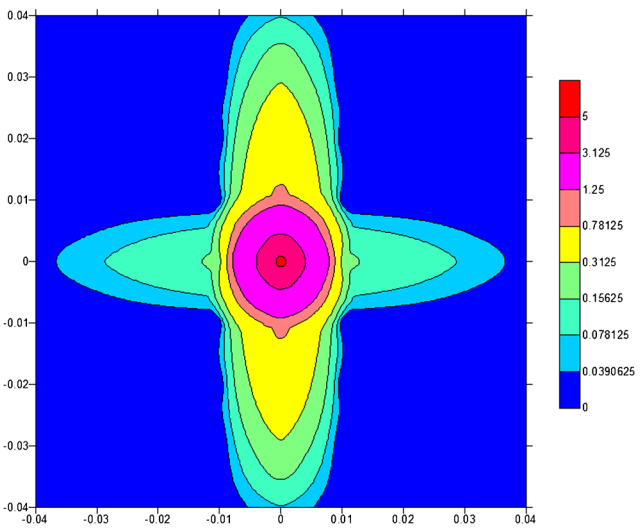

Figure 4 Simulated diffraction pattern of a strain induced twin pattern at $T < T_c$. The colour scheme refers to the amplitude of the structure factor (after Ref. [32]. Copyright (2012), AIP Publishing LLC).

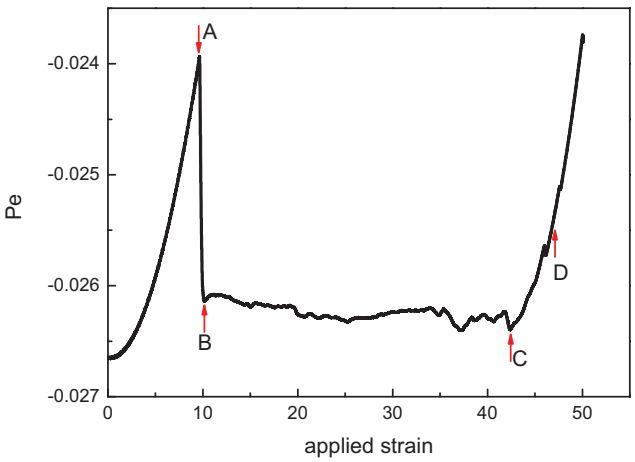

Figure 5 Time evolution under constant shear rate for the microstructure in Fig. 3. The increase of elastic energy below the yield point A is reduced with respect to the initial parabolic increase. This regime represents the formation of pre-yield tweed structures. The high twin boundary regime beyond the lower yield point B shows serration and an overall constant potential energy. This regime refers to the domain glass. The evolution is partially smooth and partially jerky. The jerks are extracted from the potential energy P_e by differentiation. The curve is taken at a temperature of 1.25 T_{VF} and we see that the unstable domain in the elastic regime collapses into a multitude of twinned nanodomains over a very small strain regime (from point A to B). When the applied strain reaches point C the detwinning process is almost complete, and finally the system changes to a perfect single domain crystal after point D (after Ref. [37], with permission from Springer Science and Business Media).

The shape of the diffraction pattern is similar to that depicted in Fig. 1 but contains more highly confined diffraction maxima along the elastically soft directions. The complexity of the underlying pattern is comparable to that of tweed while thermal excitations are much reduced.

The time evolution of the potential energy for the twin pattern at constant strain rates is shown in Fig. 5 [37]. Changes of the microstructure occur by small jerks when needle domains retract and kinks inside walls propagate. These movements generate energy 'jerks' which correspond in non-equilibrium thermodynamics to 'avalanches'. The glass state is now defined by the statistical distribution of the jerk dynamics: continuous propagation of twin boundaries under weak fields leads to no jerks. The domain dynamics can become very slow near the transition point and at low temperatures and domain freezing becomes possible. Athermal nucleation of twinning and their elimination at low temperatures corresponds to a power law statistics of the avalanche distribution. At higher temperatures, thermal excitations lead to a Vogel–Fulcher distribution of avalanches and this regime corresponds to a 'domain-glass' in the sense that the domain sub-system displays glassy behaviour. The phase diagram of the domain formation was derived by Ref. [35]. We propose hence that domain-glass states exist in regime (c) in Fig. 6. Further work is planned to confirm this idea.

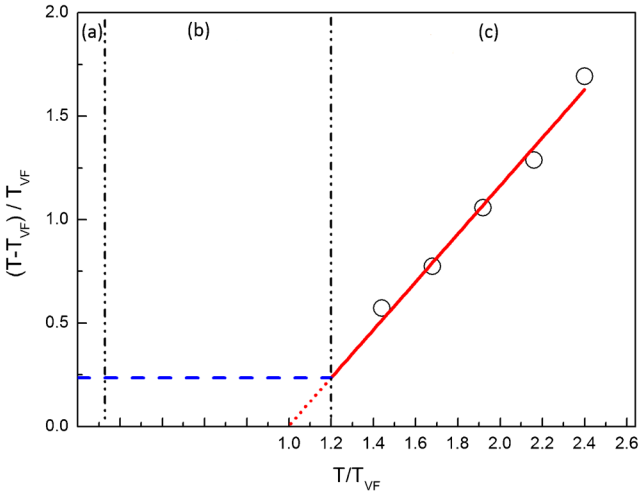

Figure 6 Phase diagram of the jerk distribution statistics. A crossover between a power law statistics (low temperatures phase b) and a Vogel–Fulcher regime (c) occurs at 1.2 T_{VF} where the temperature difference with the Vogel–Fulcher temperature increases linearly (after Ref. [35]. Copyright (2011) by the American Physical Society).

Acknowledgements E.K.H.S. is grateful to EPSRC (RG66344) and the Leverhulme Foundation (RG66640) for financial support.

References

[1] L. Cross, in: Piezoelectricity, Springer Series in Materials Science, Vol. 114 (Springer, Berlin/Heidelberg, 2008), pp. 131–155.
[2] J. Hemberger, P. Lunkenheimer, R. Fichtl, H. A. K. von Nidda, V. Tsurkan, and A. Loidl, Nature **434**(7031), 364 (2005).
[3] W. Kleemann, J. Mater. Sci. **41**(1), 129 (2006).
[4] D. Wang, Y. Wang, Z. Zhang, and X. Ren, Phys. Rev. Lett. **105**, 205702 (2010).
[5] P. Lloveras, T. Castán, A. Planes, and A. Saxena, in: Disorder and Strain-Induced Complexity in Functional Materials, edited by T. Kakeshita, T. Fukuda, A. Saxena, and A. Planes, Springer Series in Materials Science Vol. 148 (Springer, Berlin/Heidelberg, 2012), pp. 227–247.
[6] E. K. H. Salje, ChemPhysChem **11**, 940 (2010).
[7] E. Salje and H. Zhang, Phase Transit. **82**, 452 (2009).
[8] S. E. Lerner, M. Mierzwa, M. Paluch, Y. Feldman, and P. B. Ishai, J. Chem. Phys. **138**, 204501 (2013).
[9] R. J. Harrison, S. A. T. Redfern, and E. K. H. Salje, Phys. Rev. B **69**, 144101 (2004).
[10] W. T. Coffey, Y. P. Kalmykov, and S. V. Titov, in: Fractional Rotational Diffusion and Anomalous Dielectric Relaxation in Dipole Systems (John Wiley & Sons, Inc., 2006), pp. 285–437.
[11] O. Aktas, E. K. H. Salje, S. Crossley, G. I. Lampronti, R. W. Whatmore, N. D. Mathur, and M. A. Carpenter, Phys. Rev. B **88**, 174112 (2013).
[12] W. Schranz, A. Fuith, P. Dolinar, H. Warhanek, M. Haluska, and H. Kuzmany, Phys. Rev. Lett. **71**, 1561 (1993).
[13] E. Salje, U. Bismayer, B. Wruck, and J. Hensler, Phase Transit. **35**, 61 (1991).
[14] H. Xu, P. J. Heaney, and G. H. Beall, Am. Mineral. **85**, 971 (2000).
[15] M. A. Carpenter, R. E. A. McKnight, C. J. Howard, Q. Zhou, B. J. Kennedy, and K. S. Knight, Phys. Rev. B **80**, 214101 (2009).
[16] S. N. Achary, R. Mishra, O. D. Jayakumar, S. K. Kulshreshtha, and A. K. Tyagi, J. Solid State Chem. **180**(1), 84 (2007).
[17] S. Qin, A. I. Becerro, F. Seifert, J. Gottsmann, and J. Jiang, J. Mater. Chem. **10**, 1609 (2000).
[18] M. A. Carpenter and E. K. H. Salje, Eur. J. Mineral. **10**(4), 693 (1998).
[19] E. K. H. Salje, Annu. Rev. Mater. Res. **42**, 265 (2012).
[20] J. D. Axe and G. Shirane, Phys. Rev. B **1**, 342 (1970).
[21] M. A. Carpenter, A. Buckley, P. A. Taylor, R. E. A. McKnight, and T. W. Darling, J. Phys.: Condens. Matter **22**, 035406 (2010).
[22] W. Cao and G. R. Barsch, Phys. Rev. B **38**, 7947 (1988).
[23] E. K. H. Salje and H. Zhang, J. Phys.: Condens. Matter **21**, 035901 (2009).
[24] J. F. Scott, E. K. H. Salje, and M. A. Carpenter, Phys. Rev. Lett. **109**, 187601 (2012).
[25] E. K. H. Salje, M. A. Carpenter, G. F. Nataf, G. Picht, K. Webber, J. Weerasinghe, S. Lisenkov, and L. Bellaiche, Phys. Rev. B **87**, 014106 (2013).
[26] O. Aktas, M. A. Carpenter, and E. K. H. Salje, Appl. Phys. Lett. **103**, 142902 (2013).
[27] R. Pirc and R. Blinc, Phys. Rev. B **70**, 134107 (2004).
[28] S. Marais, V. Heine, C. Nex, and E. Salje, Phys. Rev. Lett. **66**, 2480 (1991).
[29] K. Parlinski, V. Heine, and E. K. H. Salje, J. Phys.: Condens. Matter **5**, 497 (1993).
[30] E. Salje and K. Parlinski, Supercond. Sci. Technol. **4**, 93 (1991).
[31] W. W. Schmahl, A. Putnis, E. Salje, P. Freeman, A. Graeme-Barber, R. Jones, K. K. Singh, J. Blunt, P. P. Edwards, J. Loram, and K. Mirza, Philos. Mag. Lett. **60**, 241 (1989).
[32] E. K. H. Salje, X. Ding, Z. Zhao, and T. Lookman, Appl. Phys. Lett. **100**, 222905 (2012).
[33] A. M. Bratkovsky, V. Heine, and E. K. H. Salje, Philos. Trans. R. Soc. A **354**, 2875 (1996).
[34] L. Goncalves-Ferreira, S. A. T. Redfern, E. Atacho, and E. K. H. Salje, Appl. Phys. Lett. **94**, 081903 (2009).
[35] E. K. H. Salje, X. Ding, Z. Zhao, T. Lookman, and A. Saxena, Phys. Rev. B **83**, 104109 (2011).
[36] X. Ding, T. Lookman, Z. Zhao, A. Saxena, J. Sun, and E. K. H. Salje, Phys. Rev. B **87**, 094109 (2013).
[37] X. Ding, T. Lookman, E. Salje, and A. Saxena, JOM **65**, 401 (2013).
[38] E. Salje, Phys. Rep. **215**, 49 (1992).
[39] A. L. Roytburd, J. Appl. Phys. **83**, 239 (1998).
[40] E. K. H. Salje, M. C. Gallardo, J. Jiménez, F. J. Romero, and J. del Cerro, J. Phys.: Condens. Matter **10**, 5535 (1998).
[41] E. K. H. Salje, X. Ding, and Z. Zhao, Appl. Phys. Lett. **102**, 152909 (2013).

